Journal of Power Sources 295 (2015) 149–155

Contents lists available at ScienceDirect

Journal of Power Sources

journal homepage: www.elsevier.com/locate/jpowsour

Lithium-ion polymer cells assembled with a reactive composite separator containing vinyl-functionalized SiO_2 particles

Ji-Hyun Yoo, Won-Kyung Shin, Sang Man Koo, Dong-Won Kim*

Department of Chemical Engineering, Hanyang University, Seongdong-Gu, Seoul 133-791, Republic of Korea

HIGHLIGHTS

- Reactive SiO_2 particles are synthesized and coated onto polyethylene separator.
- In-situ cross-linking with reactive separator allows strong interfacial adhesion.
- The cells with reactive composite separator exhibit excellent cycling performance.

ARTICLE INFO

Article history:
Received 15 April 2015
Received in revised form
30 May 2015
Accepted 30 June 2015
Available online 11 July 2015

Keywords:
Reactive composite separator
Vinyl-functionalized SiO_2
In-situ cross-linking
Lithium-ion polymer cells
Thermal stability

ABSTRACT

Vinyl-functionalized SiO_2 particles of different sizes are synthesized and coated onto both sides of a polyethylene separator to prepare a reactive composite separator for lithium-ion polymer cells. The SiO_2-coated composite separators exhibit excellent thermal stability due to the presence of heat-resistant silica particles. By using these reactive composite separators and a gel electrolyte precursor, lithium-ion polymer cells composed of a graphite negative electrode and a $LiNi_{1/3}Co_{1/3}Mn_{1/3}O_2$ positive electrode are assembled by in-situ chemical cross-linking, and their cycling performance is evaluated. The cells assembled with a reactive composite separator exhibit superior cycling performance to cell prepared with a conventional polyethylene separator due to the strong interfacial adhesion between the electrodes and separator, as well as suppression of deleterious reactions during cycling.

1. Introduction

Rechargeable lithium-ion batteries (LIBs) dominate the power source market for portable electronic devices due to their high energy density and long cycle life, and new applications such as electric vehicles and energy storage systems are gradually emerging onto the market [1–6]. In these LIBs, a separator is a critical component that prevents physical contact of the positive and negative electrodes while permitting ion transport within the cell. Proper selection of the separator is very important for achieving good battery performance and ensuring battery safety [7]. Most of the separators currently used in LIBs are based on microporous polyolefin membranes, such as polyethylene (PE) and polypropylene (PP), because of their excellent mechanical strength and good chemical stability [7,8]. However, these polyolefin separators usually exhibit high thermal shrinkage at high temperatures, which may cause an internal short circuit in cases of unusual heat generation [9–11]. Furthermore, the large difference in polarity between hydrophobic polyolefin separator and polar organic solvents leads to poor wettability, which results in high ionic resistance [12,13]. To overcome these problems, extensive studies have been carried out on surface coating of the polyolefin separator with inorganic materials such as Al_2O_3 and SiO_2 [14–20]. Although such ceramic coatings have been effective in improving the mechanical, thermal and electrical properties of polyolefin separators, ceramic particles can be detached from the separator and act as insulators to increase the internal resistance during cycling. Moreover, it is difficult to maintain good interfacial contact between the ceramic-coated separator and electrodes during cycling. In our previous studies, we synthesized reactive SiO_2 particles with C=C double bonds, which permitted surface reaction with vinyl monomers through free radical polymerization [21–25]. The coating of vinyl-functionalized SiO_2 particles onto the polyolefin separator and the in-situ cross-linking using these reactive SiO_2 particles are of great interest because the thermal stability of the polymer

* Corresponding author.
E-mail address: dongwonkim@hanyang.ac.kr (D.-W. Kim).

http://dx.doi.org/10.1016/j.jpowsour.2015.06.156
0378-7753/

separator and the electrode-electrolyte interfacial contacts can be greatly enhanced by the combined effect of incorporating ceramic particles with high thermal resistance and thermal cross-linking induced by reactive SiO_2 particles.

In this study, we synthesized vinyl-functionalized SiO_2 particles with different sizes and uniformly coated them onto both sides of a PE separator. Due to the presence of heat-resistant SiO_2 particles, the silica-coated separators exhibited excellent thermal stability. The reactive composite separator was applied to the cell composed of a graphite negative electrode and a $LiNi_{1/3}Co_{1/3}Mn_{1/3}O_2$ positive electrode, and an in-situ cross-linking reaction was then induced after injecting an electrolyte solution containing a small amount of tri(ethylene glycol) diacrylate (TEGDA), as schematically demonstrated in Fig. 1. The cycling performance of the lithium-ion polymer cells was evaluated and compared to those of a cell assembled with a pristine PE separator.

2. Experimental

2.1. Synthesis of vinyl-functionalized SiO_2 particles

Vinyl-functionalized SiO_2 particles were synthesized by sol–gel reaction of vinyltrimethoxysilane (VTMS) in an aqueous solution, as previously reported [21–25]. An appropriate amount of VTMS (Evonik) was added to double-distilled water while stirring until the VTMS droplets were completely disappeared. A catalytic amount of NH_4OH in water (28 wt.%, Junsei) was added to the solution, and the sol–gel reaction was allowed to proceed for 12 h at ambient temperature. After reaction completion, the resulting precipitate was centrifuged and washed several times with ethanol. The SiO_2 particle size was controlled by changing the concentration of VTMS. Vinyl-functionalized SiO_2 particles with diameters ranging from 300 to 900 nm were obtained as a white powder after vacuum drying at 110 °C for 12 h.

2.2. Preparation of reactive composite separator

The coating solution was prepared by mixing the vinyl-functionalized SiO_2 particles and poly(vinylidene fluoride-co-hexafluoropropylene) (P(VdF-co-HFP), Kynar 2801) in a mixed solvent of acetone/butanol (90/10 by volume) using ball milling for 12 h. The weight ratio of SiO_2 particle to P(VdF-co-HFP) was 70:30. When the mixture was completely homogenized, the resulting solution was applied to both sides of the PE separator (SK Innovation Co.), which was 9 μm thick and had a porosity of 40%. The SiO_2-coated separator was dried at room temperature for 30 min to allow the solvent to evaporate, followed by additional drying in a vacuum oven at 80 °C for 24 h.

2.3. Electrode preparation and cell assembly

The positive electrode was prepared by coating an N-methyl pyrrolidine (NMP)-based slurry containing 85.0 wt.% $LiNi_{1/3}Co_{1/3}Mn_{1/3}O_2$ (3 M Co.), 7.5 wt.% poly(vinylidene fluoride) (PVdF), and 7.5 wt.% super-P carbon (MMM Co.) onto an aluminum foil. Its active mass loading corresponded to a capacity of about 2.0 mAh cm^{-2}. The negative electrode was prepared similarly by coating an NMP-based slurry of mesocarbon microbeads (MCMB, Osaka gas), PVdF, and super-P carbon (88:8:4 by weight) onto a copper foil. To prepare a gel electrolyte precursor solution, 3.5 wt.% of TEGDA (Sigma–Aldrich) was added to the liquid electrolyte with t-amyl peroxypivalate (Seki Arkema) as a thermal radical initiator. A liquid electrolyte consisting of 1.15 M $LiPF_6$ in ethylene carbonate (EC)/ethylmethyl carbonate (EMC)/diethyl carbonate (DEC) (3:5:2 by volume, battery grade) was kindly supplied by PANAX ETEC Co. Ltd. and was used without further treatment. A lithium-ion polymer cell was assembled by sandwiching a reactive composite separator between the graphite negative electrode and the $LiNi_{1/3}Co_{1/3}Mn_{1/3}O_2$ positive electrode. The cell was enclosed in a pouch injected with gel electrolyte precursor and was then vacuum-sealed. After cell assembly, the cells were stored at 70 °C for 1 h in order to induce in-situ chemical cross-linking within the cell. For comparison, a liquid electrolyte-based lithium-ion cell with a pristine PE separator and the same liquid electrolyte was also assembled.

2.4. Characterization and measurements

The morphologies of vinyl-functionalized SiO_2 particles and separators were examined using a field emission scanning electron microscope (FE-SEM, JEOL JSM-6330F). The thermal shrinkage of PE separator and SiO_2-coated separators was measured in terms of dimensional changes after being held for 30 min at 55 and 130 °C, respectively. Fourier transform infrared (FT-IR) spectra were recorded on a JASCO 760 IR spectrometer in the range of 400–2400 cm^{-1}. Charge and discharge cycling tests of the lithium-ion polymer cells were conducted at a current density of 1.0 mA cm^{-2} (0.5 C rate) over the voltage range from 3.0 to 4.5 V using battery test equipment (WBCS 3000, Wonatech). AC impedance measurements were performed using a Zahner Electrik IM6 impedance analyzer over a frequency range of 100 kHz–1 mHz with an amplitude of 10 mV at 25 °C. Surface characterization of the graphite negative electrode in the cell after 100 cycles at 55 °C was conducted using X-ray photoelectron spectroscopy (XPS). The electrode was washed several times with anhydrous dimethyl carbonate to remove residual electrolyte, followed by vacuum drying overnight at room temperature. XPS measurements were

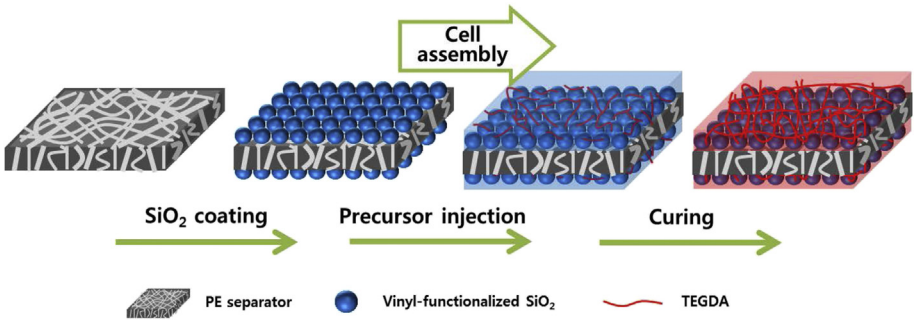

Fig. 1. Schematic illustration of the preparation of cross-linked composite separator using reactive SiO_2 particles and gel electrolyte precursor containing TEGDA.

conducted on a Thermo VG Scientific ESCA 2000 system using an Al Kα radiation source. HF content in the electrolyte was measured using an acid–base titration method after the cell was stored in a 55 °C oven for three days [26]. Methyl orange (Sigma–Aldrich) was used as an acid–base indicator.

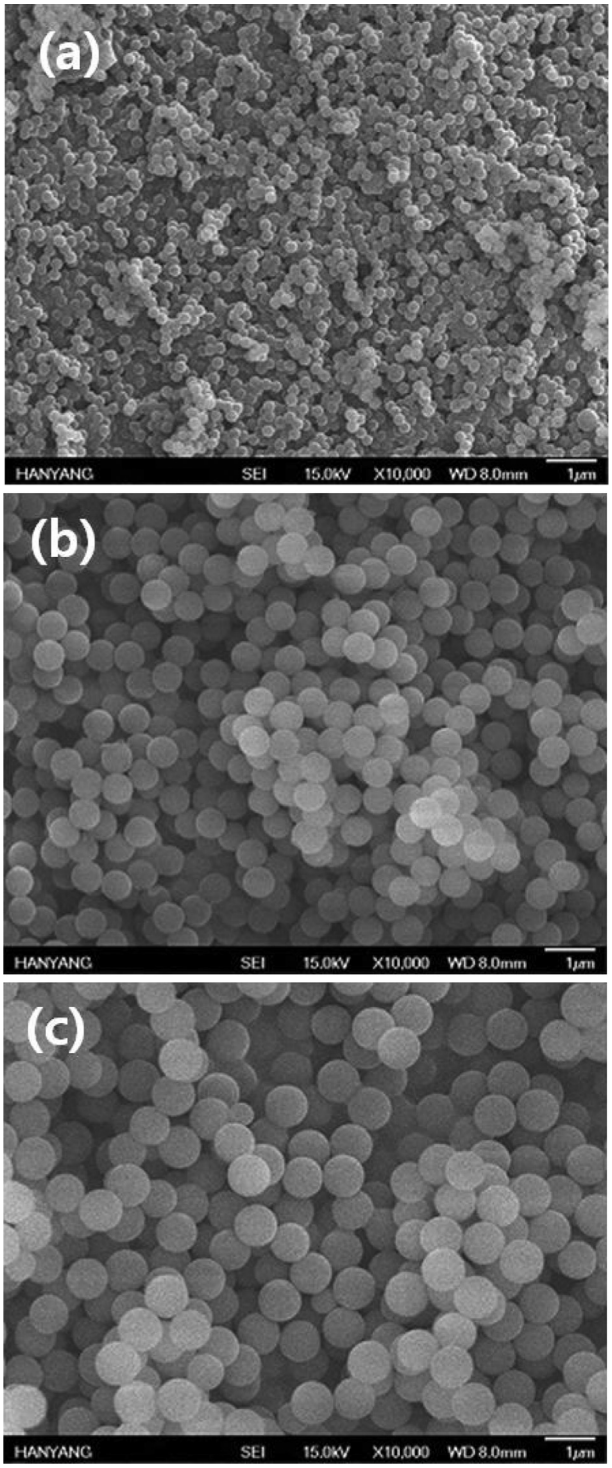

Fig. 2. SEM images of vinyl-functionalized SiO_2 particles with different diameters of (a) 300 nm, (b) 600 nm and (c) 900 nm.

3. Results and discussion

Fig. 2 shows the FE-SEM images of vinyl-functionalized SiO_2 particles obtained through the sol–gel reaction of VTMS in an aqueous solution. All silica particles had uniform spherical shapes with average diameters of about 300, 600, and 900 nm, respectively. The SiO_2 particles synthesized were coated onto both sides of a PE separator. The FE-SEM images of the pristine PE separator and SiO_2 (particle size: 300 nm)-coated PE separator are presented in Fig. 3. The PE separator showed a uniform submicron pore structure. When the vinyl-functionalized SiO_2 particles were coated onto the PE separator, they were uniformly distributed on the surface in order to provide cross-linking sites throughout the composite separator. Since SiO_2 particles contain many reactive vinyl groups on their surface, they participate in radical polymerization with TEGDA during the in-situ cross-linking process, which prevents silica particles from detaching from the separator. The thickness of the reactive SiO_2-coated separator was approximately 12 μm.

Because the manufacturing process of the PE separators includes biaxial stretching, they readily lose dimensional stability upon exposure to high temperatures around their melting temperature (~135 °C). Thus, it is very important to maintain their dimension at high temperatures for preventing the electric short circuit between electrodes, the failure of which may eventually lead to fire or explosion under unusual conditions such as abnormal

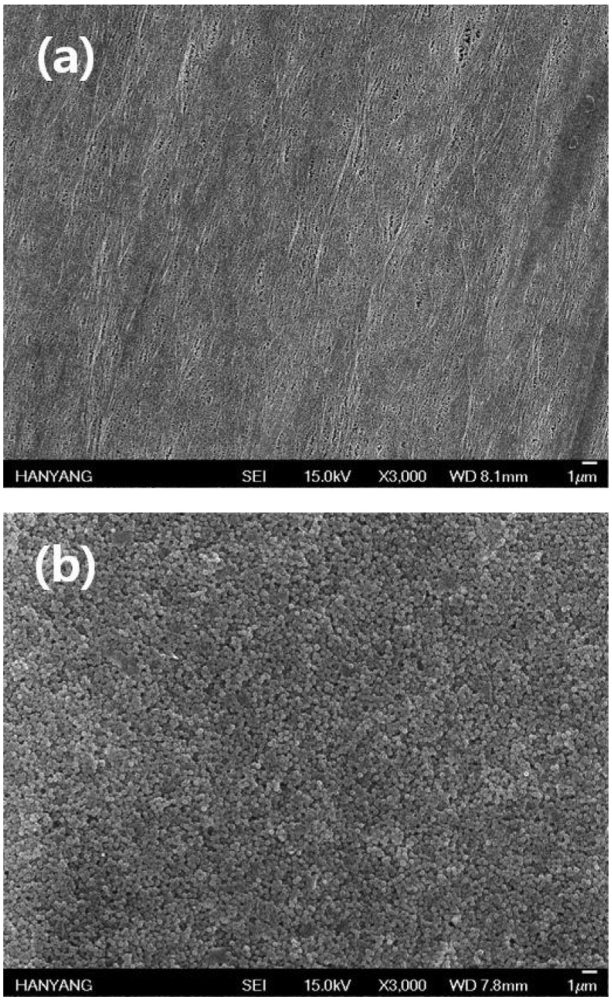

Fig. 3. SEM images of (a) PE separator and (b) reactive SiO_2 (particle size: 300 nm)-coated PE separator (RCS-300).

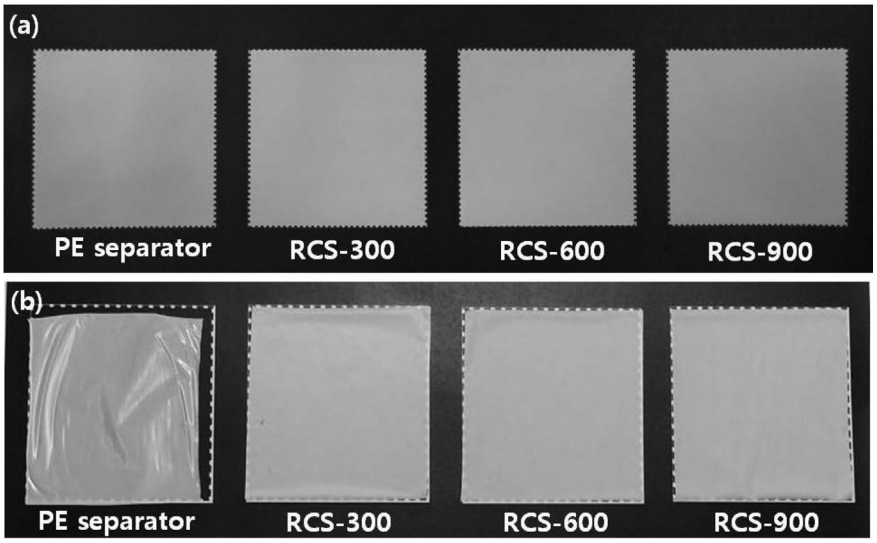

Fig. 4. Photographs of PE separator and reactive composite separators after exposure for 30 min at (a) 55 °C and (b) 130 °C. In this figure, RCS-300 represents a reactive composite separator coated by reactive SiO_2 particles with a diameter of 300 nm.

heating and mechanical rupture. To evaluate the thermal stability of pristine PE and reactive composite separators, we measured thermal shrinkage after holding them for 30 min at 55 and 130 °C, respectively; the results are shown in Fig. 4. At 55 °C, there are no significant differences in their dimension, indicating they are dimensionally stable at that temperature. However, the pristine PE separator experienced a high degree of shrinkage (11.2%) during high-temperature (130 °C) exposure. In contrast, the PE separators coated with SiO_2 particles did not show any thermal shrinkage regardless of SiO_2 particle size when exposed to the same conditions. This result is attributed to the incorporation of thermally-resistant SiO_2 particles onto both sides of the PE separator, helping to prevent thermal shrinkage of the separator at high temperature.

Before cell assembly, FT-IR analysis was carried out to confirm the chemical cross-linking reaction between vinyl-functionalized SiO_2 particles and TEGDA, and the resulting FT-IR spectra are shown in Fig. 5(a). As depicted in this figure, the vinyl-functionalized SiO_2 particles showed characteristic peaks corresponding to the asymmetric stretching vibrations of Si—O—Si around 1100 cm^{-1}. The presence of reactive C=C double bonds in the SiO_2 particles was confirmed by two peaks at 1412 and 1600 cm^{-1}. These peaks are characteristic of C=C double bonds [27,28], indicating that the SiO_2 particles contained vinyl groups, allowing free radical reactions with TEGDA in the gel electrolyte precursor. The peaks observed at 1725 and 1636 cm^{-1} for TEGDA were assigned to the carbonyl groups and the C=C double bond, respectively [29]. The FT-IR spectrum of the cross-linked composite separator revealed no peaks corresponding to C=C double bonds in the SiO_2 particles. This result suggests that vinyl groups on the surface of SiO_2 particles react with TEGDA to form a cross-linked composite separator through free radical polymerization. Fig. 5(b) shows the FE-SEM image of the cross-linked composite separator synthesized by thermal curing with a reactive composite separator and gel electrolyte precursor at 70 °C for 1 h. As shown in the figure, the PE separator was fully covered with a cross-linked composite gel layer. The composite gel layer was formed by cross-linking between vinyl-functionalized SiO_2 particles on a PE separator and TEGDA in the gel electrolyte precursor, as schematically illustrated

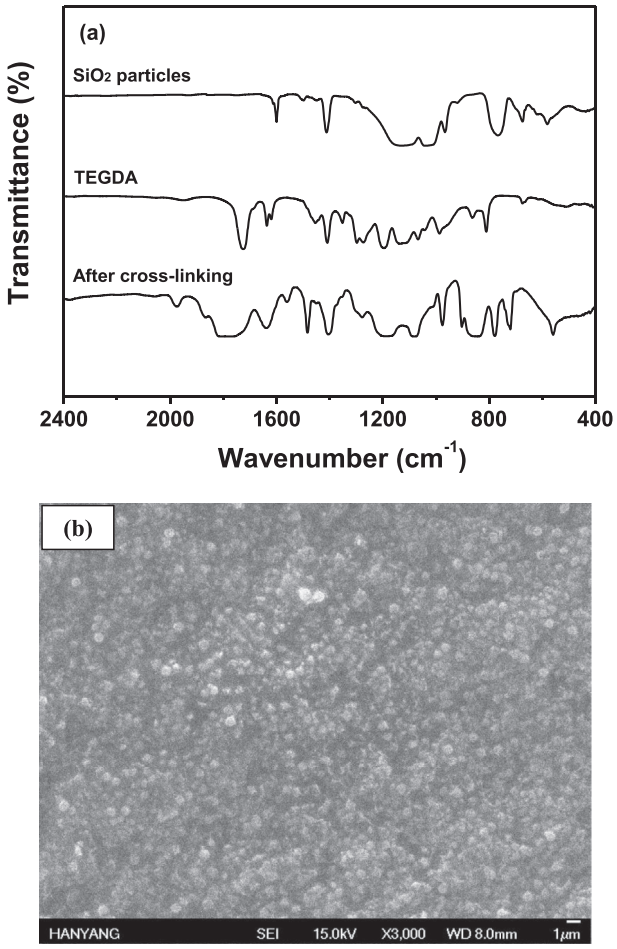

Fig. 5. (a) FT-IR spectra of vinyl-functionalized SiO_2 particles, TEGDA and cross-linked composite separator synthesized by thermal curing with reactive SiO_2 particles and gel electrolyte precursor, and (b) FE-SEM image of cross-linked composite separator.

in Fig. 1. The electrolyte solution was well encapsulated in the cross-linked composite gel layer without leakage of organic solvents.

We evaluated the cycling performance of lithium-ion polymer cells assembled by in-situ cross-linking reaction with the reactive composite separator and gel electrolyte precursor. The cells were initially subjected to a preconditioning cycle in the voltage range of 3.0–4.5 V at a constant current rate of 0.1 C. After two cycles at 0.1 C, the cells were charged at a current density of 0.5 C up to a cut-off voltage of 4.5 V. This was followed by a constant-voltage charge with decreasing current until a final current equal to 10% of the charging current was obtained. The cells were then discharged to a cut-off voltage of 3.0 V at the same current density. Fig. 6(a) shows the charge and discharge curves of the 1st, 50th, 100th, 200th and 300th cycles of a lithium-ion polymer cell assembled with a reactive SiO_2(300 nm)-coated separator (RCS-300). The cell had an initial discharge capacity of 178.7 mAh g^{-1} based on the active $LiNi_{1/3}Co_{1/3}Mn_{1/3}O_2$ material in the positive electrode. After 300 cycles, it delivered a discharge capacity of 160.9 mAh g^{-1}, corresponding to 90.0% of the initial discharge capacity. Fig. 6(b) shows the discharge capacities of lithium-ion polymer cells assembled with different separators as a function of cycle number. For the purpose of comparison, the cycling results of the cell assembled with a pristine PE separator and liquid electrolyte are also shown. The cycling characteristics of the cells were found to depend on the type of separator. The initial discharge capacity of the cell was slightly decreased when using reactive composite separators. A cross-linking reaction induced by reactive SiO_2 particles on a PE separator may inevitably increase the resistance of ion migration between the two electrodes, resulting in a reduction in discharge capacity. With respect to cycling stability, the cells assembled with a reactive composite separator exhibited better capacity retention than the cell with a pristine PE separator. Upon in-situ cross-linking reaction between reactive SiO_2 particles and gel electrolyte precursor, the cross-linked gel formed on a PE separator can serve as an adhesive, chemically bonding the separator and the electrodes,

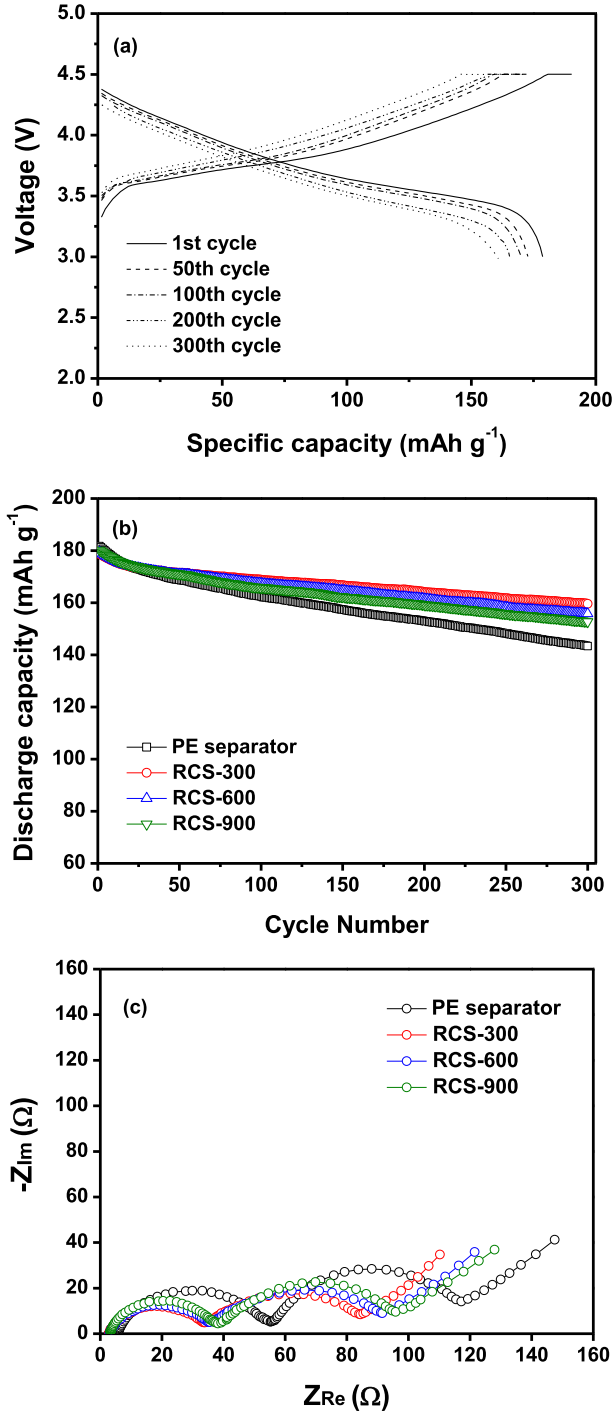

Fig. 6. (a) Charge and discharge curves of a lithium-ion polymer cell assembled with reactive composite separator (300 nm SiO_2), (b) discharge capacities of lithium-ion polymer cells assembled with different separators (0.5 C CC and CV charge, 0.5 C CC discharge, cut-off: 3.0–4.5 V, 25 °C) and (c) AC impedance spectra of lithium-ion polymer cells assembled with different separators, which are measured after 300 cycles at 25 °C.

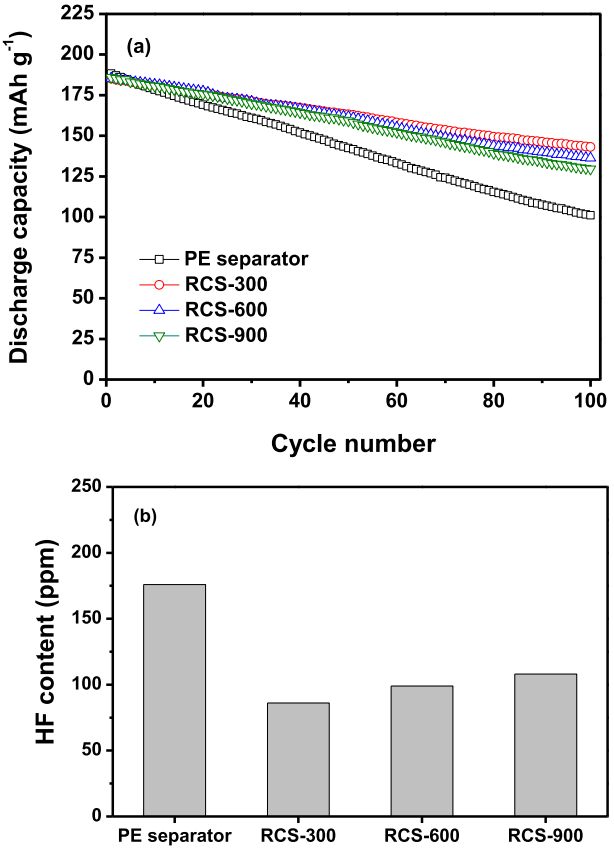

Fig. 7. (a) Discharge capacities of lithium-ion polymer cells assembled with different separators at 55 °C (0.5 C CC and CV charge, 0.5 C CC discharge, cut-off: 3.0–4.5 V), and (b) HF contents in the cells with different separators after storage at 55 °C for three days.

which results in strong interfacial contacts. In particular, the presence of vinyl-functionalized SiO_2 particles with small particle size and large surface area enabled increased cross-linking and more effective encapsulation of liquid electrolyte, resulting in good cycling stability. Accordingly, the cell assembled with a reactive composite separator containing SiO_2 particles with a diameter of 300 nm exhibited the best capacity retention. To understand the effect of SiO_2 particle size on the cycling performance of the cells, AC impedance spectra were collected in a charged state for each type of cell after 300 cycles, and the results are shown in Fig. 6(c). All spectra exhibited two overlapping semicircles due to different interfacial resistance contributions. The first semicircle in the higher frequency range is attributed to resistance due to Li^+ ion migration through the surface film on the electrodes (R_f), and the second semicircle in the middle to low frequency range arises from charge transfer resistance at the electrode-electrolyte interface (R_{ct}) [30–32]. The electrolyte resistance estimated from the intercept on the real axis in the high-frequency range was highest in the cell employing a pristine PE separator. This result can be ascribed to loss of electrolyte solution due to poor wettability of the PE separator and deleterious reactions between the organic solvents and electrodes. It is notable that the cell employing reactive SiO_2 particles with a particle size of 300 nm had the lowest interfacial resistances after 300 cycles. In this cell, the cross-linked composite gel layer formed between the PE separator and electrodes enabled effective trapping of the electrolyte solution and reduced the deleterious reactions between organic solvents and electrodes. It is also plausible that, as the degree of cross-linking increases, the interfacial bonding between the electrodes and the separator becomes stronger; this is essential for efficient charge transport during charge–discharge cycling. These features ultimately limited growth of the resistive layer on electrode surface and enhanced interfacial stability. As a result, the cell with reactive SiO_2 particles with a particle size of 300 nm exhibited the most stable cycling performance, as shown in Fig. 6(b).

Fig. 7(a) shows the discharge capacities of the lithium-ion polymer cells assembled with different separators as a function of cycle number, obtained at 55 °C and 0.5 C rate. The cells delivered initial discharge capacities ranging from 185.2 to 188.3 mAh g^{-1}, which were higher than those obtained at 25 °C. The capacity retention was remarkably improved through the incorporation of reactive composite separators. It is well known that layered $LiNi_xCo_yMn_{1-x-y}O_2$ materials show capacity fading at high temperatures due to structural and interfacial instabilities as well as dissolution

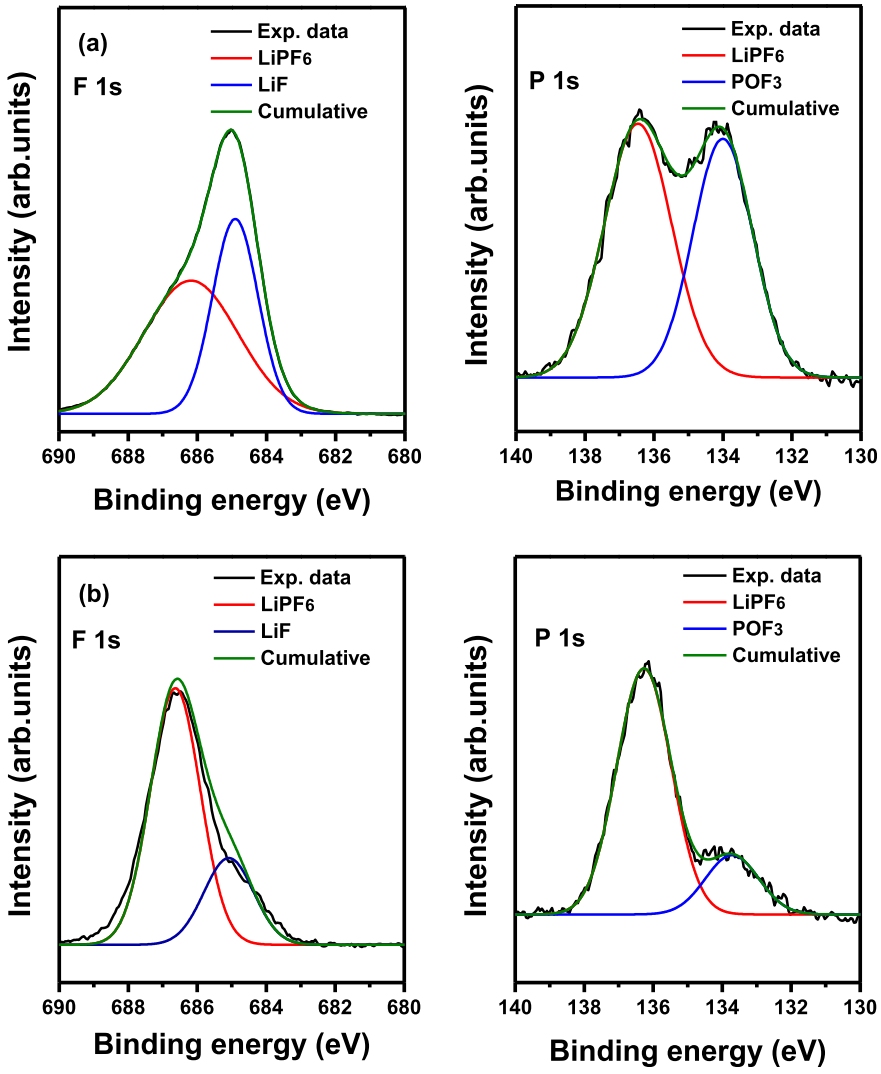

Fig. 8. F 1s and P 1s XPS spectra of graphite electrodes in the lithium-ion polymer cells assembled with (a) PE separator and (b) RCS-300 after 100 cycles at 55 °C.

of transition metals from the active cathode material due to HF attack [33,34]. HF is known to be generated by thermal decomposition and hydrolysis of $LiPF_6$ by trace moisture in the electrolyte solution [35,36]. Fig. 7(b) shows the HF concentrations in the cells with different separators, which were measured after storing the cells at 55 °C for three days. Clearly, the HF content was significantly reduced in the cells with SiO_2-coated separators. The SiO_2 particles on the reactive composite separator can serve as HF scavengers to remove HF in the electrolyte solution as a result of formation of strong chemical bonds (Si–F) by nucleophilic substitution reaction of HF, as previously reported [37,38]. Accordingly, the use of a SiO_2-coated separator reduced HF content and suppressed the dissolution of transition metals from the active $LiNi_{1/3}Co_{1/3}Mn_{1/3}O_2$ material at elevated temperatures. In the cell employing liquid electrolyte with a PE separator, the dissolution of transition metals by HF attack possibly caused a rapid increase in interfacial resistance, thereby accelerating capacity loss as cycling progressed at elevated temperatures.

The surface of the graphite negative electrodes in cells with a pristine PE separator and SiO_2(300 nm)-coated separator was analyzed by means of XPS after 100 cycles at 55 °C, and the results are shown in Fig. 8. In the F 1s XPS spectra, the relative peak intensity of LiF at 685.1 eV [39,40] was much higher on the electrode surface of the cell with the pristine PE separator. It is well known that LiF is produced by the thermal decomposition of $LiPF_6$ salt on the electrode surface [35]. It is an insulating material for both electrons and Li^+ ions, and thus LiF that forms on the surface of the electrode may hamper the charge transfer reaction between the electrode and the electrolyte, thereby increasing the charge transfer resistance. In the P 1s XPS spectra, the intensity of the peak corresponding to POF_3 (134.0 eV), another species generated by the decomposition of $LiPF_6$, was also higher on the graphite electrode of the cell with a pristine PE separator. These XPS results suggest that the in-situ cross-linking reaction using a reactive SiO_2-coated separator was very effective in suppressing electrolyte decomposition at high temperature, which is consistent with the cycling results shown in Fig. 7(a).

4. Conclusions

Vinyl-functionalized SiO_2 particles of different sizes were synthesized and coated on both sides of a PE separator in order to prepare a reactive composite separator. These separators exhibited enhanced thermal stability by retaining stable dimensions at high temperature. The vinyl-functionalized SiO_2 particles on PE separator participated in free radical polymerization with TEGDA in a gel electrolyte precursor. An in-situ cross-linking reaction using reactive SiO_2-coated separators promoted strong interfacial adhesion between electrodes and separator, and allowed effective encapsulation of liquid electrolyte, resulting in low interfacial resistances. Lithium-ion polymer cells employing the reactive composite separators exhibited good cycling stability at both ambient and elevated temperatures. Thus, it is expected that the reactive SiO_2-coated separators will be useful as separators for rechargeable lithium-ion polymer cells, which require good cycling stability and enhanced thermal safety.

Acknowledgments

This work was supported by a grant from the National Research Foundation of Korea funded by the Korean government (MEST) (NRF-2009-C1AAA001-0093307) and by a grant from the Human Resources Development Program of KETEP, funded by the Ministry of Trade, Industry and Energy of Korea (No. 20124010203290).

References

[1] M. Winter, R.J. Brodd, Chem. Rev. 104 (2004) 4245–4269.
[2] A.S. Arico, P. Bruce, B. Scrosati, J.-M. Tarascon, W.V. Schalkwijk, Nat. Mater. 4 (2005) 366–377.
[3] B. Dunn, H. Kamath, J.-M. Tarascon, Science 334 (2011) 928–935.
[4] V. Etacheri, R. Marom, R. Elazari, G. Salitra, D. Aurbach, Energy Environ. Sci. 4 (2011) 3243–3262.
[5] B. Scrosati, J. Hassoun, Y.K. Sun, Energy Environ. Sci. 4 (2011) 3287–3295.
[6] D. Larcher, J.-M. Tarascon, Nat. Chem. 7 (2015) 19–29.
[7] S.S. Zhang, J. Power Sources 164 (2007) 351–364.
[8] P. Arora, Z. Zhang, Chem. Rev. 104 (2004) 4419–4462.
[9] G. Venugopal, J. Moore, J. Howard, S. Pendalwar, J. Power Sources 77 (1999) 34–41.
[10] I. Uchida, H. Ishikawa, M. Mohamedi, M. Umeda, J. Power Sources 119–121 (2003) 821–825.
[11] M.S. Wu, P.C.J. Chiang, J.C. Lin, Y.S. Jan, Electrochim. Acta 49 (2004) 1803–1812.
[12] J. Saunier, F. Alloin, J.Y. Sanchez, G. Caillon, J. Power Sources 119–121 (2003) 454–459.
[13] Y.M. Lee, J.W. Kim, N.S. Choi, J.A. Lee, W.H. Seol, J.K. Park, J. Power Sources 139 (2005) 235–241.
[14] H.R. Jung, D.H. Ju, W.J. Lee, X. Zhang, R. Kotek, Electrochim. Acta 54 (2009) 3630–3637.
[15] H.S. Jeong, D.W. Kim, Y.U. Jeong, S.Y. Lee, J. Power Sources 195 (2010) 6116–6121.
[16] J.A. Choi, S.H. Kim, D.W. Kim, J. Power Sources 195 (2010) 6192–6196.
[17] Y.S. Lee, Y.B. Jeong, D.W. Kim, J. Power Sources 195 (2010) 6197–6201.
[18] J. Fang, A. Kelarakis, Y.W. Lin, C.Y. Kang, M.H. Yang, C.L. Cheng, Y. Wang, E.P. Giannelis, L.D. Tsai, Phys. Chem. Chem. Phys. 13 (2011) 14457–14461.
[19] H. Xiang, J. Chen, Z. Li, H. Wang, J. Power Sources 196 (2011) 8651–8655.
[20] W.K. Shin, D.W. Kim, J. Power Sources 226 (2013) 54–60.
[21] Y.S. Lee, S.H. Ju, J.H. Kim, S.S. Hwang, J.M. Choi, Y.K. Sun, H. Kim, B. Scrosati, D.W. Kim, Electrochem. Commun. 17 (2012) 18–21.
[22] S.H. Ju, Y.S. Lee, Y.K. Sun, D.W. Kim, J. Mater. Chem. A 1 (2013) 395–401.
[23] Y.S. Lee, J.H. Lee, J.A. Choi, W.Y. Yoon, D.W. Kim, Adv. Funct. Mater. 23 (2013) 1019–1027.
[24] W.K. Shin, Y.S. Lee, D.W. Kim, J. Mater. Chem. A 2 (2014) 6863–6869.
[25] S.M. Park, Y.S. Lee, D.W. Kim, J. Electrochem. Soc. 162 (2015) A3071–A3076.
[26] Y.K. Sun, K.J. Hong, J. Prakash, K. Amine, Electrochem. Commun. 4 (2002) 344–348.
[27] J.P. Blitz, R.S.S. Murthy, D.E. Leyden, J. Colloid Interface Sci. 121 (1988) 63–69.
[28] P. Siberzan, L. Leger, D. Ausserre, J.J. Benattar, Langmuir 7 (1991) 1647–1651.
[29] A. Ghadimi, M. Amirilargani, T. Mohammadi, N. Kasiri, B. Sadatnia, J. Membr. Sci. 458 (2014) 14–26.
[30] M.D. Levi, G. Salitra, B. Markovsky, H. Teller, D. Aurbach, U. Heider, L. Heider, J. Electrochem. Soc. 146 (1999) 1279–1289.
[31] Y. Bai, X. Wang, X. Zhang, H. Shu, X. Yang, B. Hu, Q. Wei, H. Wu, Y. Song, Electrochim. Acta 109 (2013) 355–364.
[32] T. Liu, A. Garsuch, F. Chesneau, B.L. Lucht, J. Power Sources 269 (2014) 920–926.
[33] G.G. Amatucci, J.M. Tarascon, L.C. Klein, Solid State Ionics 83 (1996) 167–173.
[34] S.U. Woo, B.C. Park, C.S. Yoon, S.T. Myung, J. Prakash, Y.K. Sun, J. Electrochem. Soc. 154 (2007) A649–A655.
[35] H. Yang, G.V. Zhuang, P.N. Ross Jr., J. Power Sources 161 (2006) 573–579.
[36] E. Zinigrad, L. Larush-Asraf, J.S. Gnanaraj, M. Sprecher, D. Aurbach, Thermochim. Acta 438 (2005) 184–191.
[37] T. Yim, H.J. Ha, M.S. Park, K.J. Kim, J.S. Yu, Y.J. Kim, RSC Adv. 3 (2013) 25657–25661.
[38] W. Cho, S.M. Kim, J.H. Song, T. Yim, S.G. Woo, K.W. Lee, J.S. Kim, Y.J. Kim, J. Power Sources 282 (2015) 45–50.
[39] D. Aurbach, I. Weissman, A. Schechter, Langmuir 12 (1996) 3991–4007.
[40] D. Aurbach, K. Gamolsky, B. Markovsky, Y. Gofer, M. Schmidt, U. Heider, Electrochim. Acta 47 (2002) 1423–1439.